Laser surface alloying of aluminium (AA1200) with Ni and SiC powders

L.A.B. Mabhali[a,b*], S.L. Pityana[a], N. Sacks[b]
[a]Council for Scientific and Industrial Research - National Laser Centre, P O Box 395, Bld 46F, Pretoria, South Africa, 0001
[b]School of Chemical and Metallurgical Engineering, University of the Witwatersrand, Private Bag 3, Wits, South Africa, 2050
* Corresponding author: Email address: lmabhali@csir.co.za

Abstract

An Nd:YAG laser was used for surface alloying of aluminium AA1200. The alloying powder was a mixture of Ni and SiC in different ratios. A study of the microstructures obtained after alloying was conducted using optical and scanning electron microscopy. EDX and XRD were used for phase identification. Analysis of the alloyed layer revealed the presence of Al_4C_3, $AlNi_3$ and α-Al-Si eutectic phases. The SiC particles dissociated into Si and C. The dissociated C reacted with Al to form Al_4C_3. The addition of Ni resulted in the formation of the Al_3Ni phase. A hardness increase of approximately 4 times that of aluminium AA1200 was achieved in the alloyed layer.

Keywords: Laser surface alloying; Metal matrix composite; Intermetallic compounds; Surface hardness; Al_4C_3

1. Introduction

Aluminium is extensively used in industry due to its low cost, light weight and excellent workability. However its low wear resistance and hardness are limiting factors in many applications. Laser alloying may be used to improve the aluminium surface properties such as hardness by modifying the composition and microstructure of the surface without affecting the bulk properties of the material [1,2,3]. This process involves melting the substrate surface and injecting powder of the alloying material into the melt pool. Process parameters such as laser power, beam spot size, laser scan speed and powder feed rate have to be controlled to achieve the desired surface properties [4].

The surface properties can be modified by adding elemental powders, thereby forming intermetallic compounds. An intermetallic compound is a solid phase consisting of two or more metallic elements in definite proportions. The intermetallic compounds generally have superior properties compared to the base aluminium such as high hardness and high wear and corrosion resistance [2,4,5]. Hard particles such as Al_3O_2, SiC, TiC and WC can also be injected into the surface of a metal matrix to improve surface properties [6-8]. In this way a surface metal matrix composite (MMC) is formed. The MMC layer has excellent hardness and wear resistance compared to the base alloy [9-13].

Su and Lei [9] laser cladded Al-12wt%Si with a powder containing SiC and Al-12wt%Si in a 3:1 volume ratio. A CO_2 laser was used with 2-4kW laser power, 2-10mm/s laser scanning speed and a 3mm diameter laser beam. The aim of the study was to form a surface MMC layer on the aluminium matrix. It was reported that the laser melting of SiC particles onto an aluminium substrate produces aluminium carbides. The presence of the Al_4C_3 phase in MMC is not desirable as it is brittle and hydroscopic. The addition of Al-12wt%Si was found to suppress or eliminate the aluminium carbides in the MMC layer. A good distribution of injected SiC particles was achieved near the surface. The microhardness of the coating was between 220 and 280 $HV_{0.1}$.

Hu and Baker [10] formed MMC layers on aluminium AA6061 alloy surfaces by incorporating SiC particles using a CO_2 laser at different energy densities. Large surface areas of MMC layers were produced by overlapping single laser tracks. The thickness of the MMC layer was dependent on the laser energy density. The microstructure and phases in the layers were also strongly dependent on the energy

density. Al_4C_3 needles, Al_4SiC_4 platelets and free Si phases were formed at nominal energy densities of 100-200MJ/m^2. The formation of Al_4C_3 needles in the MMC layer could be reduced by applying high energy densities ~560 MJ/m^2. The laser energy density is directly related to the surface temperature generated by the laser beam.

Anandkumar et al [14] conducted a detailed study of the microstructure of the aluminium MMC layers produced by a 2 kW Nd:YAG laser. The main processing parameter found to have a significant influence on the microstructure and properties of the coating was energy density. At low energy densities (~26 MJ/m^2) the SiC particles were retained and dispersed in the coating. At high specific energies (~ 58 MJ/m^2) the SiC dissolved and reacted with the molten aluminium. Analysis of the microstructure revealed small amounts of SiC dispersed near the surface along with phases such as Al_4SiC and eutectic Al-Si. The undesirable Al_4C_3 phase was completely suppressed.

Selvan et al. [16] laser alloyed aluminium AA1100 with electrodeposited nickel using a CO_2 laser. The alloying was performed with a beam diameter of 1mm using various scanning speeds and laser powers. The aim of the study was to improve the surface hardness of aluminium by forming Al-Ni intermetallic phases in the alloyed layer. The intermetallic phases formed were Al_3Ni and Al_3Ni_2. The hardness of the alloyed layers was in the range of 600-950 $HV_{0.1}$.

The objective of the present work is to evaluate the possibility of strengthening the aluminium surface by forming a composite surface layer reinforced by SiC particles as well as *in situ* generated Al-Ni intermetallic phases. Aluminium AA1200 was selected for this study due to its low cost and light weight. The aluminium AA1200 was laser alloyed with powders containing SiC and Ni in three different weight ratios. The microstructure, phases and hardness of the laser deposited thin layers were studied.

2. Experimental procedure

The laser surface alloying-particle injection was carried out using a high power Rofin Sinar Nd:YAG laser. The process parameters used in the experiments are given in Table 1. An off axis nozzle was used for powder injection. Argon was used as the shielding gas to prevent oxidation during the alloying process. The laser energy density was maintained at 200 MJ/m^2 throughout the experiments. (The laser energy density is calculated from: $E\ (MJ/m^2) = q/(r_B v)$,where q is the laser power, r_B is the radius of the laser beam and v is the laser scanning velocity).

The substrate material used in this study was aluminium AA1200 and its chemical composition is shown in Table 2. The aluminium was cut into 100x100mm^2 plates with a thickness of 6mm. The aluminium plates were sand blasted and cleaned with acetone prior to alloying.

Table 1 Laser parameters used.

Shielding gas	Argon
Shielding gas flow rate	4 L/min
Laser Power	4 kW
Powder feed rate	2 g/min
Laser beam diameter	4 mm
Laser scanning speed	10 mm/s
Energy density	200 MJ/m^2

Table 2 Chemical composition of aluminium AA1200.

Element	Cu	Si	Fe	Al
Composition (wt%)	0.12	0.13	0.59	Balance

The alloying powders used were pure Ni and SiC. These powders were weighed separately and then mixed in a vial. Weight ratios of 30wt%Ni + 70wt%SiC, 50wt%Ni + 50wt%SiC and 70wt%Ni + 30wt%SiC were selected. The powder particle morphology and size distribution were analyzed using a scanning electron microscope (SEM) and Malvern Mastersizer 2000 image analyzer. The phase compositions of the powders were identified using a P A Naytical X' Pert Pro powder diffractometer.

Cross-sections of the alloyed layers were sectioned and polished to a 1μm finish. The polished surfaces were etched using Keller's reagent. The microstructure and chemical composition of deposited layers were studied using optical and scanning electron microscopy with energy dispersive x-ray (EDX) analysis. X-ray diffraction (XRD) was used for identifying the phases formed.

The hardness measurement of the specimens was performed on polished cross sections using a Vickers microhardness tester with a load of 100g. Hardness profiles were constructed for each alloying composition depicting the hardness from the alloyed surface down to a depth of approximately 5.3mm. For the profiles the spacing between two consecutive hardness indents was 100μm.

3. Results and discussion

3.1 Materials characterization

Aluminium AA 1200 cross sections were sectioned and polished to a 1μm finish. XRD analysis was performed to determine the phases present. Figure 1 shows the XRD results of an aluminium AA1200 specimen. Only Al peaks were observed proving that the sample was pure aluminium. The hardness of aluminum AA1200 is 24.0 ± 0.4 $HV_{0.1}$.

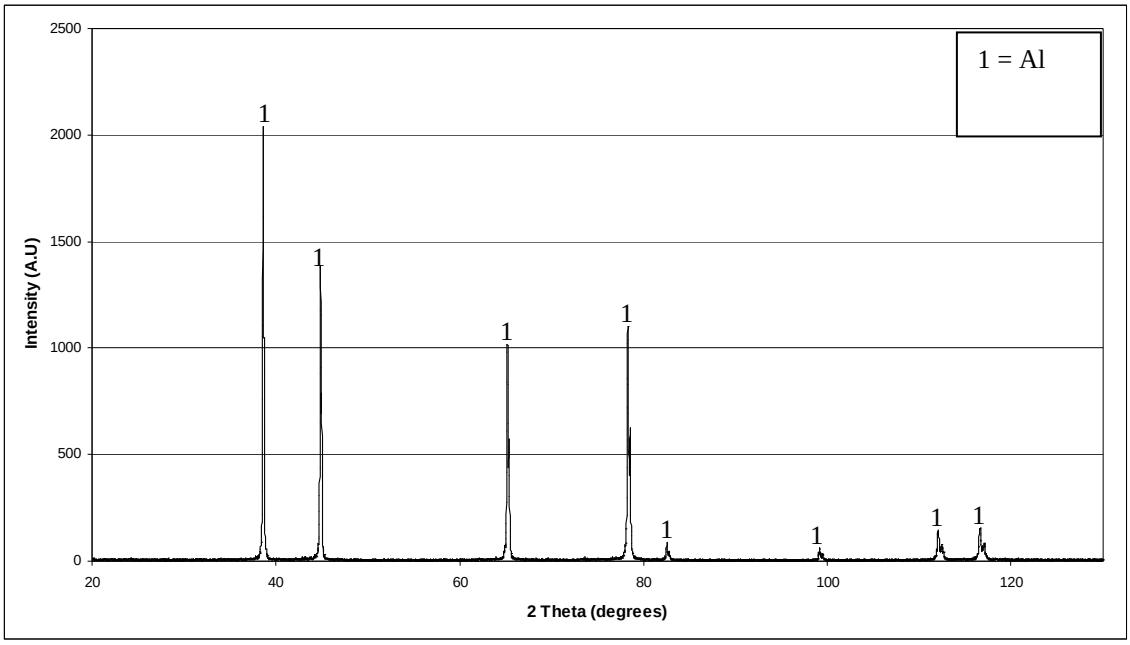

Fig. 1 XRD of Aluminum AA1200

The particle morphology of the Ni and SiC powders was investigated. The shape of the powder particles affect the manner in which the particles flow during laser processing. Round particles flow better than irregular particles. Figure 2 is an SEM micrograph of Ni powder particles showing that the powder particles are spherical and irregular. XRD results in Figure 3 show that the powders contain Ni only.

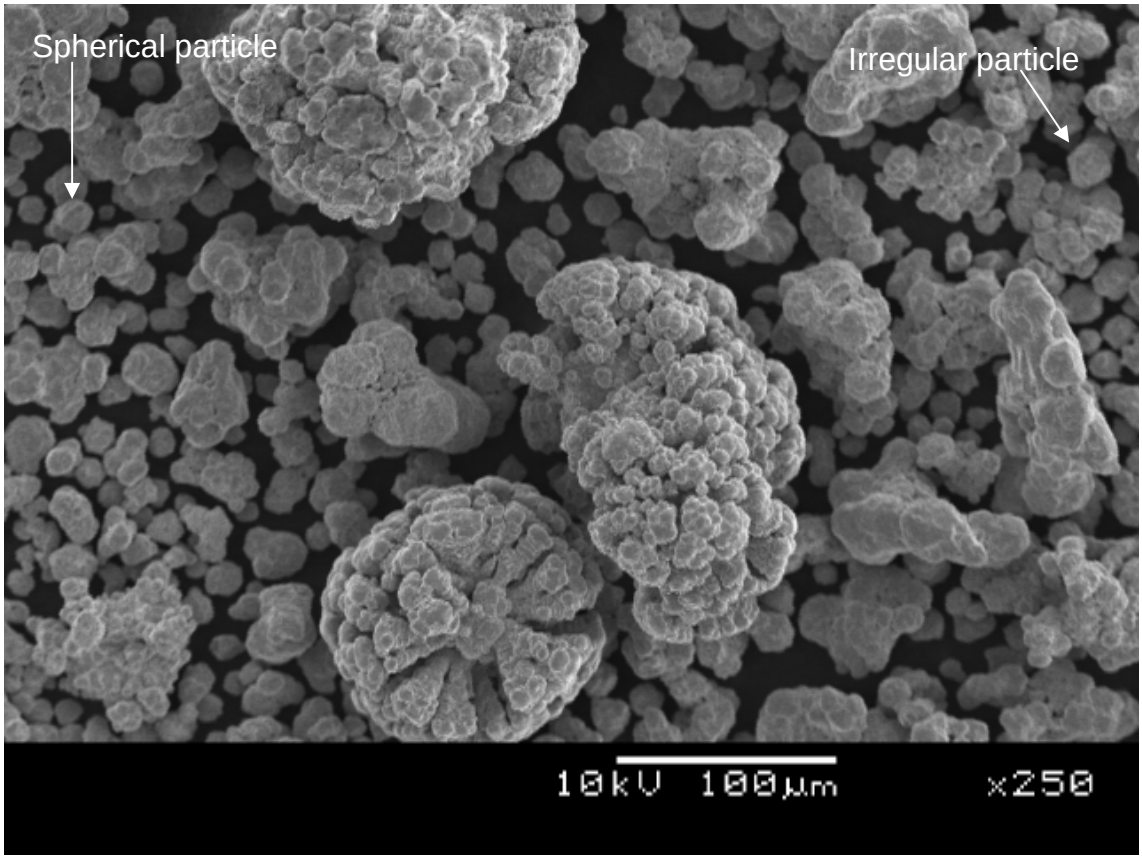

Fig. 2 SEM micrograph of Ni powder particles

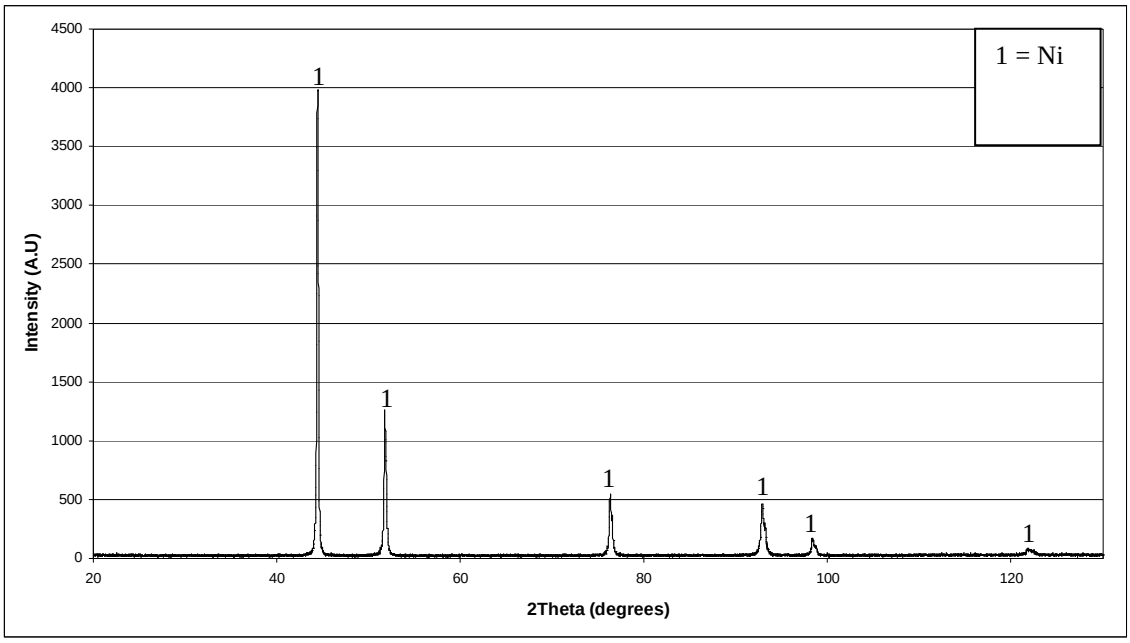

Fig. 3 XRD of Ni powder

Figure 4 is a SEM micrograph of SiC powder particles showing that the particles are irregular in shape. The particle size range was found to be wide. A large variation in particle size implies that some particles may dissolve (smaller particles) during laser processing and some will be retained (larger particles). XRD results in Figure 5 show that the powders contain SiC only.

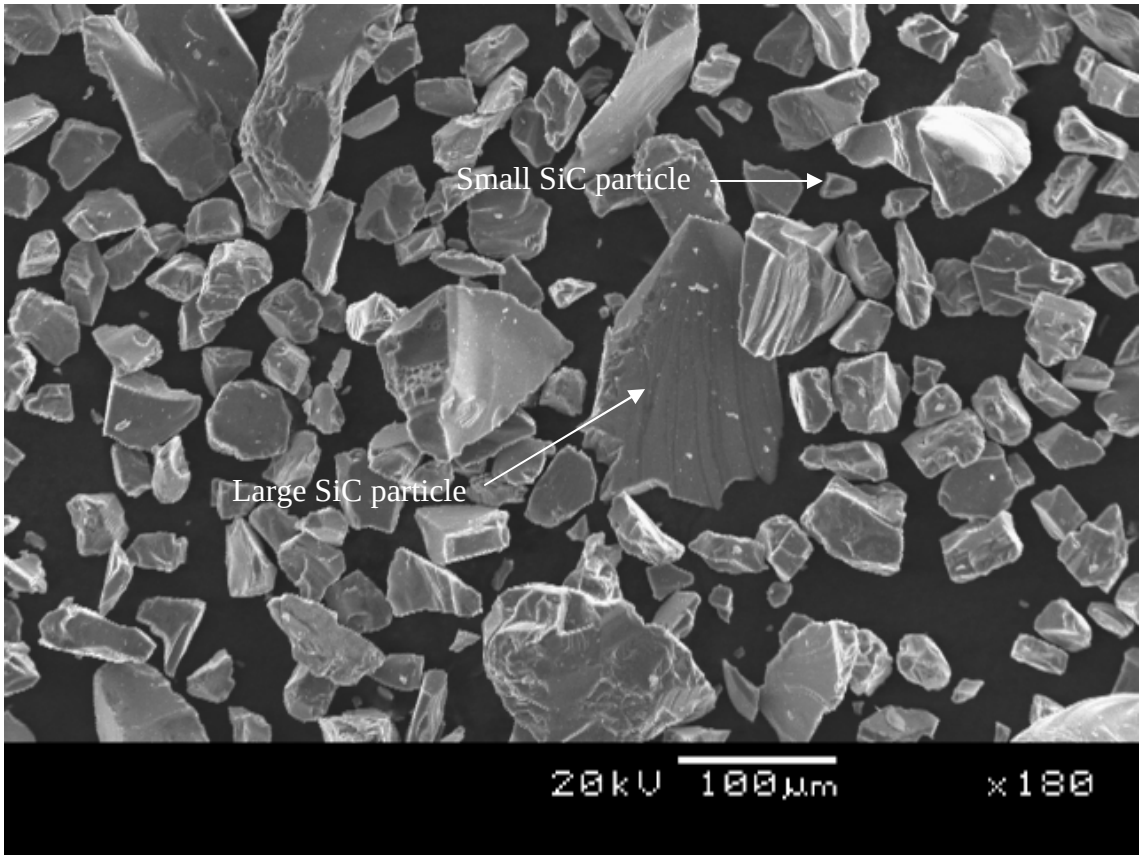

Fig. 4 SEM micrograph of SiC powder particles

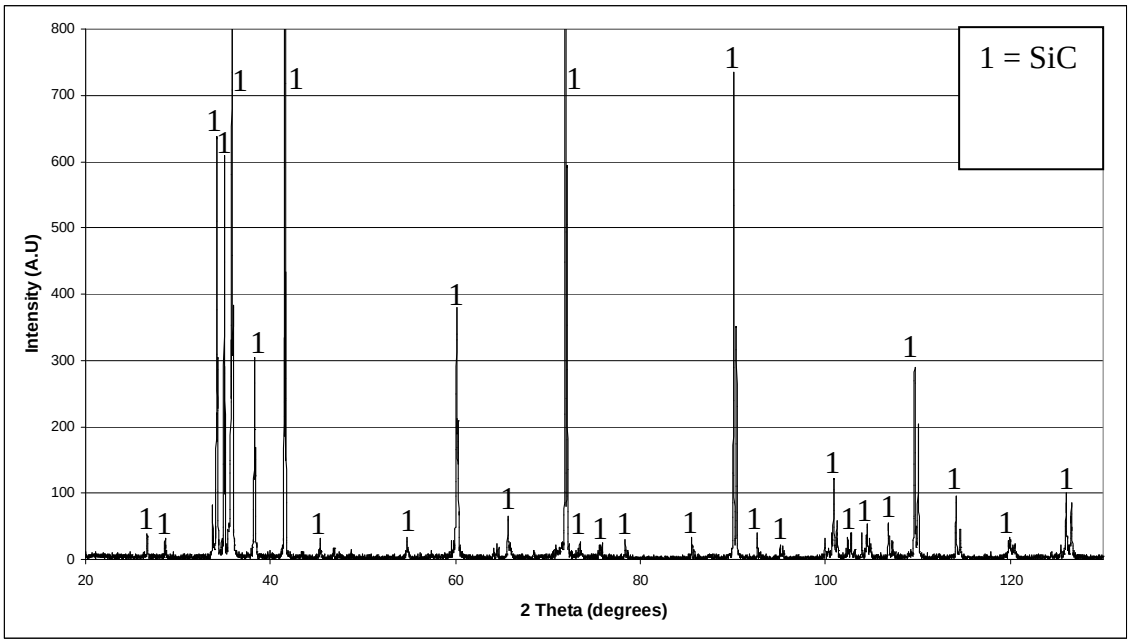

Fig. 5 XRD of SiC powder

The particle size ranges observed from the size distribution curves are 7-200 µm for Ni and 14-800 µm for SiC. Particle size distribution is important as small particles dissolve faster than larger particles.

3.2 Microstructure and composition of the alloyed materials

Figure 6 shows a typical optical micrograph of the alloyed surface for the different ratios of powder mixtures. The laser beam irradiates the powder particles and the aluminium substrate. The large differences in the melting points of Ni (1455^{o}C), SiC (2500^{o}C) and the Al alloy (582^{o}C) allow the aluminium substrate to be preferentially melted. In the present experiments, the laser energy density led to dissolution of the SiC particles with a few large particles being retained after solidification. The dissolved SiC particles and the Ni diffused into the laser generated molten aluminium through convective flow.

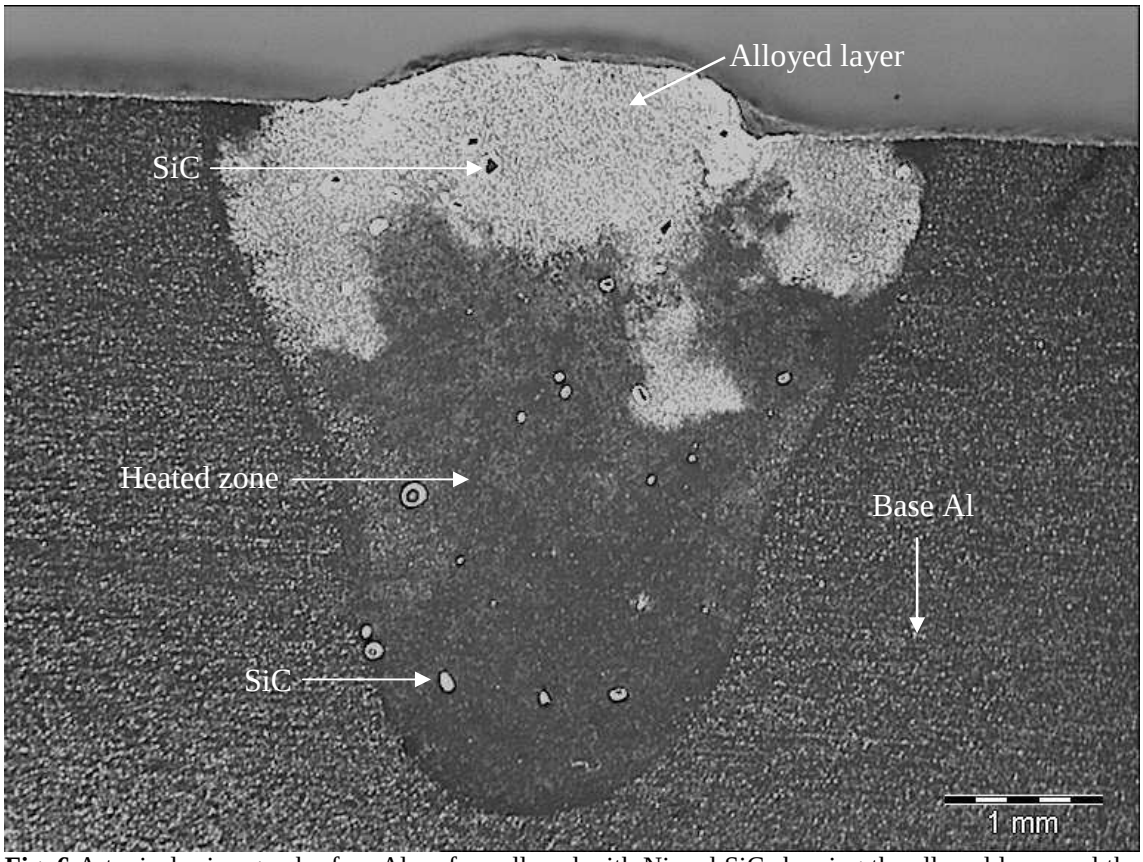

Fig. 6 A typical micrograph of an Al surface alloyed with Ni and SiC showing the alloyed layer and the heated zone

The alloyed layer is formed near the surface of the alloyed material. It consists of a homogeneous microstructure. All the Ni and most of the SiC powder particles dissolved in this region due to the high temperatures achieved. The alloyed layer is composed of few undissolved SiC particles, a dendritic Al-Ni intermetallic phase, an Al_4C_3 phase and the α-Al-Si eutectic phase. The heated zone formed below the alloyed layer. As most of the powder particles dissolved and reacted in the alloyed layer, few particles reached this region. This region was dominated by the formation of the α-Al-Si eutectic phase and melting of the Al substrate. Few SiC particles, Al_3Ni and Al_4C_3 intermetallic phases were observed in the heated zone. The Al_3Ni and Al_4C_3 intermetallic phases were generally observed in the boundary region of the heated zone and alloyed layer.

3.2.1 30wt% Ni and 70wt% SiC

The microstructure of the alloyed layer obtained when a powder mixture of 30wt%Ni and 70wt%SiC was used is shown in Figure 7. Figure 7(a) shows three different phases identified as an un-dissolved SiC particle, the Al-Ni dendritic structure and the α-Al-Si eutectic phase. In Figure 7(b), the needle-shaped phase with different orientations was identified by XRD as Al_4C_3. The Al_4C_3 phase was more dominant in the alloyed layer compared to the Al-Ni dendritic phase.

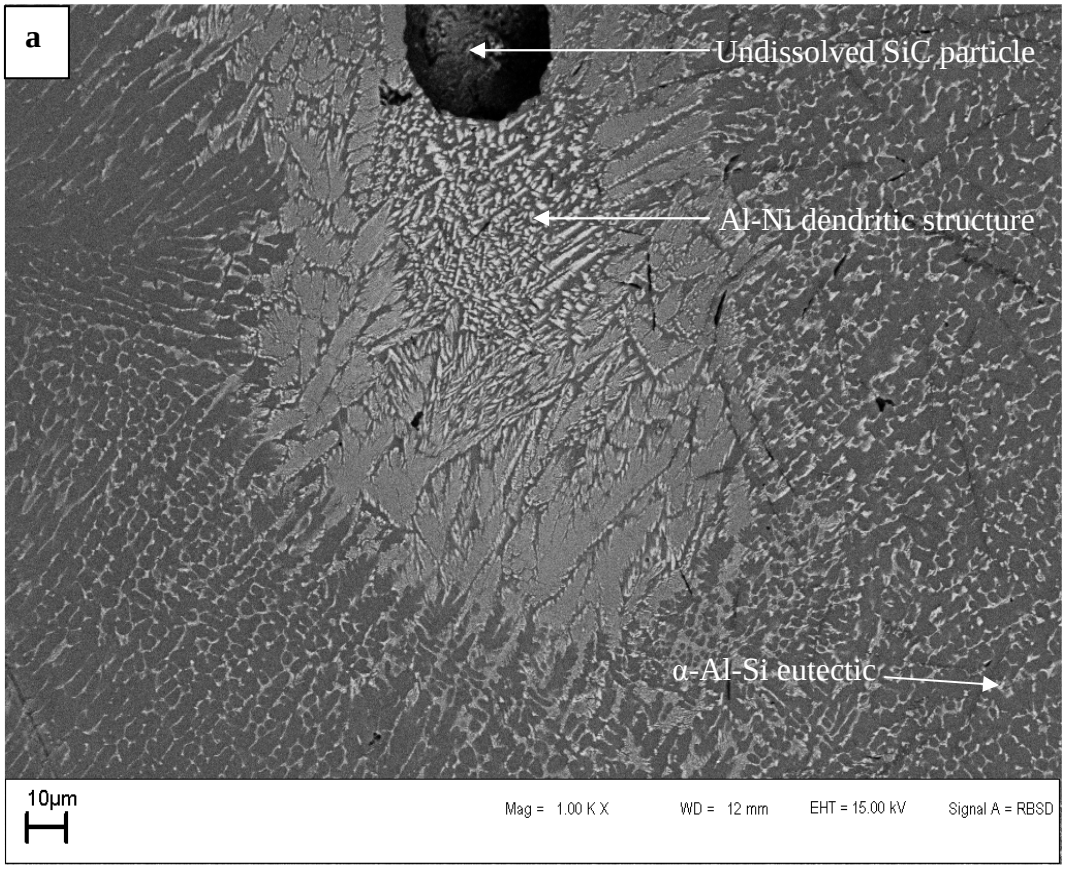

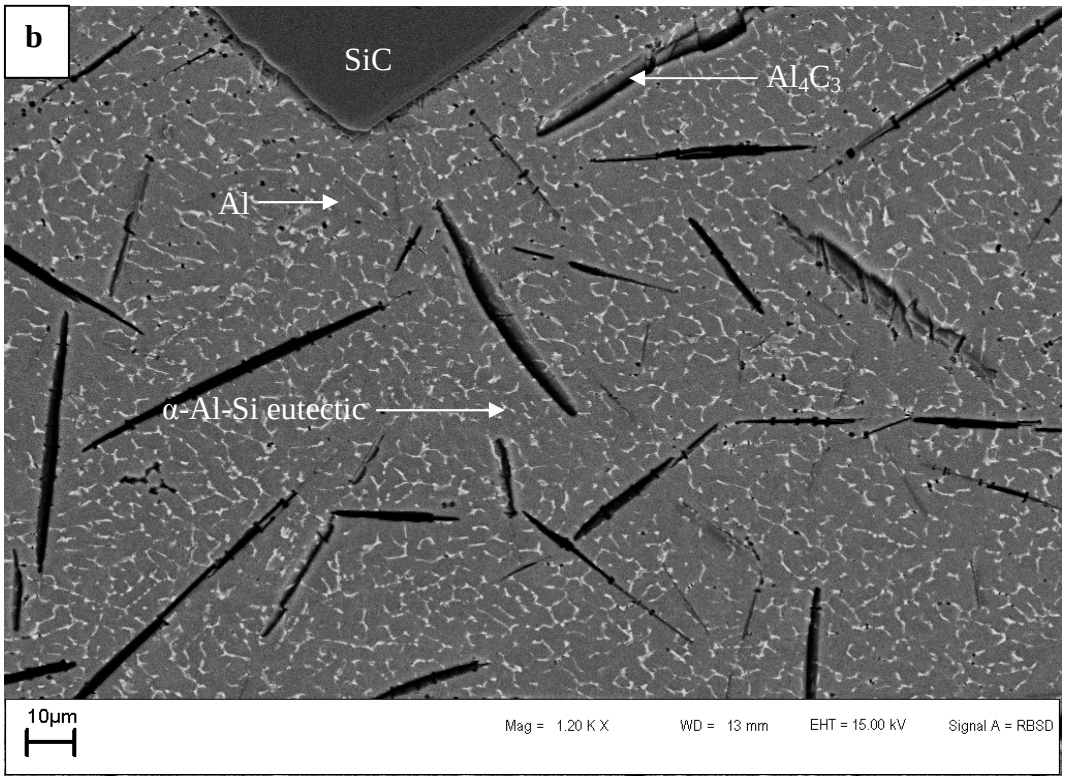

Fig. 7 SEM micrographs of alloyed layer for powder containing 30wt%Ni and 70wt%SiC showing (a) undissolved SiC particle, Al-Ni dendritic structure and α-Al-Si eutectic phase (white) and (b) SiC particle, α-Al-Si eutectic (white), Al_4C_3 needles and Al (grey)

The various phases obtained in this sample were identified by EDX and XRD (shown in Figure 8). The phases were identified as Al, SiC, Al_3Ni and Al_4C_3.

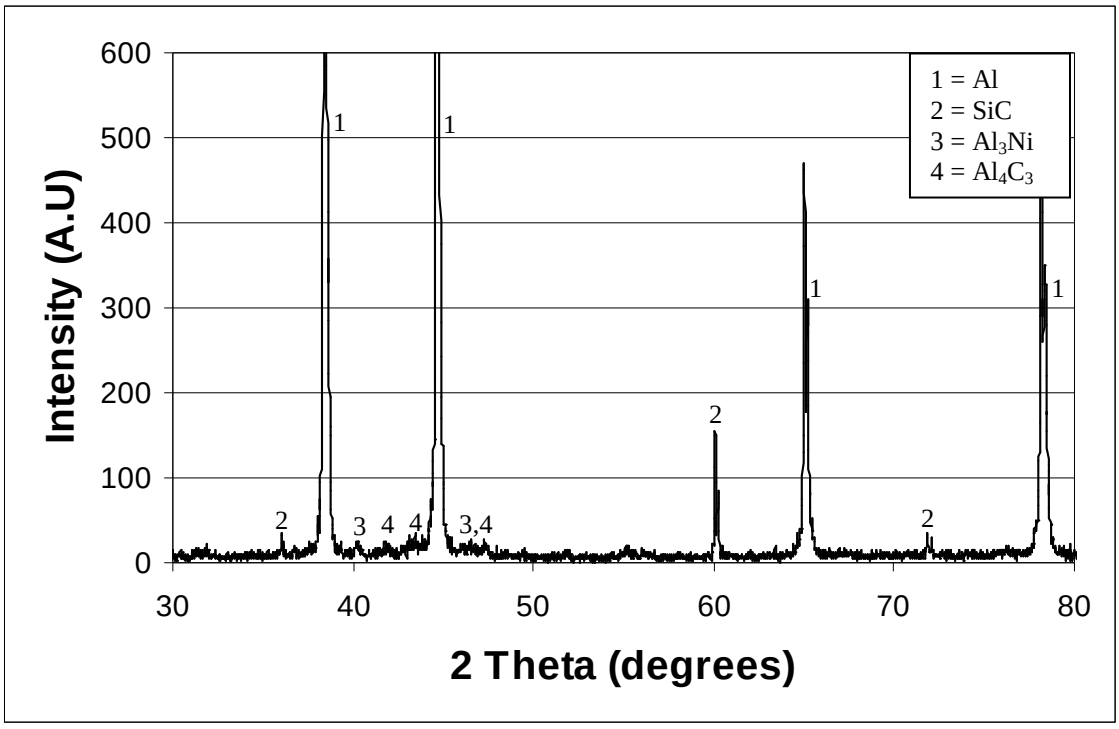

Fig. 8 XRD of an aluminium surface alloyed with 30wt%Ni and 70wt%SiC

The microstructure of the heated zone is shown in Figure 9. In this zone the microstructure is predominantly α-Al-Si eutectic. The SiC particles and Al_4C_3 phase were also observed.

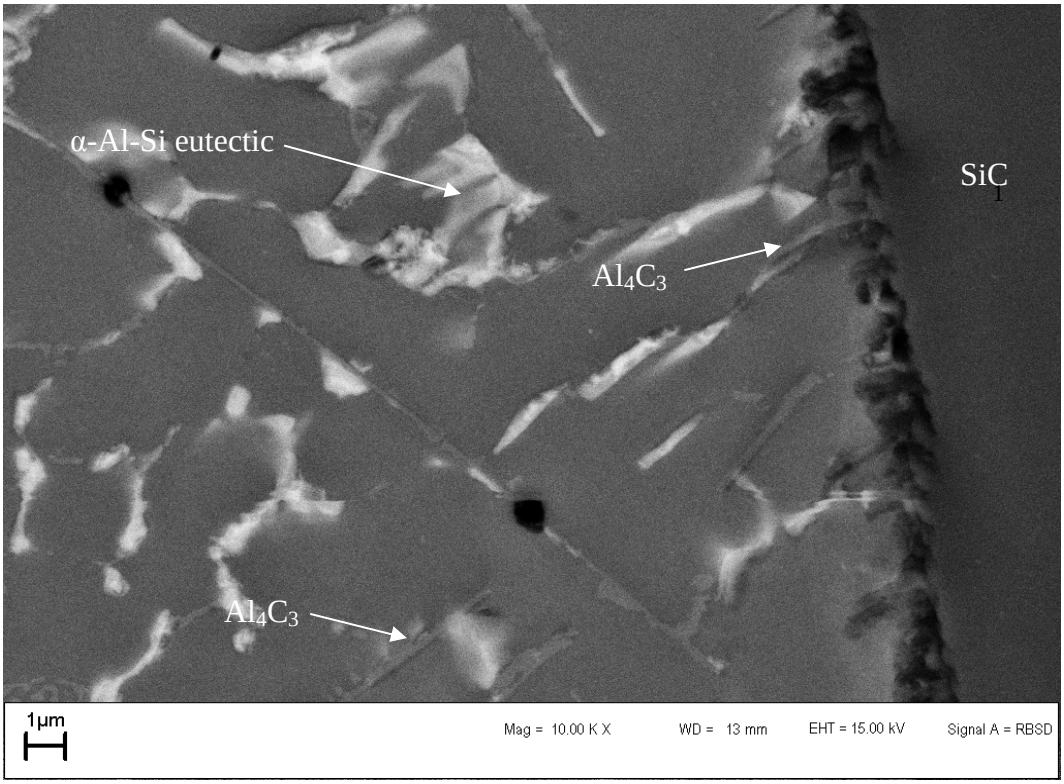

Fig. 9 SEM micrograph of heated zone for powder mixture of 30wt%Ni and 70wt%SiC showing SiC particle, Al_4C_3 and α-Al-Si eutectic phase

3.2.2 50wt%Ni and 50wt%SiC

Figure 10 shows the microstructure of the layer formed by depositing 50wt%Ni and 50wt%SiC in the aluminium matrix. The intermetallic compound Al_3Ni, shown in Figure 10(a), was synthesized *in situ* in the alloyed layer. This phase has a coarse dendritic structure. In Figure 10(b), the microstructure of the heated zone is shown. In this zone, the microstructure mainly comprises of Al_4C_3 needles and α-Al-Si eutectic surrounded by the Al matrix. These phases were also observed in the surfaces alloyed with 30wt%Ni and 70wt%SiC. There is an approximately equal amount of Al_3Ni and Al_3C_4 phases in the alloyed zone. The Al_3Ni phase content is higher in this alloy compared to alloying with 30wt%Ni and 70wt%SiC. Figure 10(c) shows the aluminum matrix in which the α-Al-Si eutectic, a few Al_3C_4 needles and an undissolved SiC particle coexist in the heated zone. The bonding between the SiC particle and the matrix appears to be deficient.

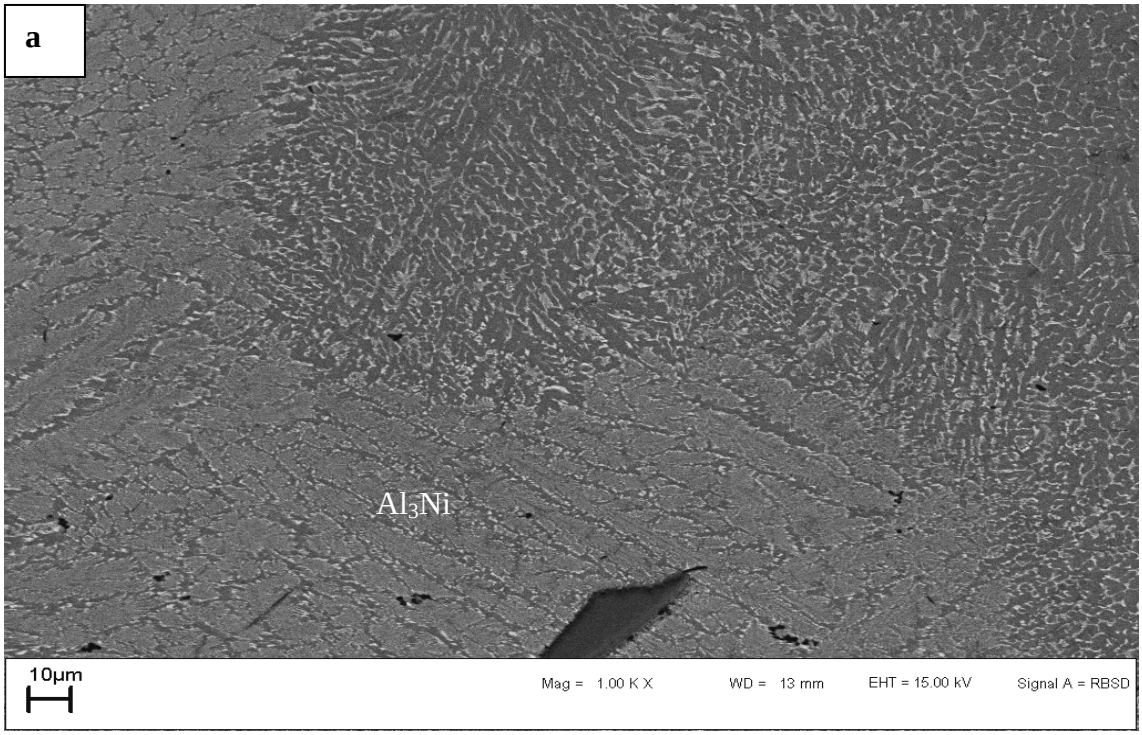
a
Al_3Ni
10µm
Mag = 1.00 K X
WD = 13 mm
EHT = 15.00 kV
Signal A = RBSD

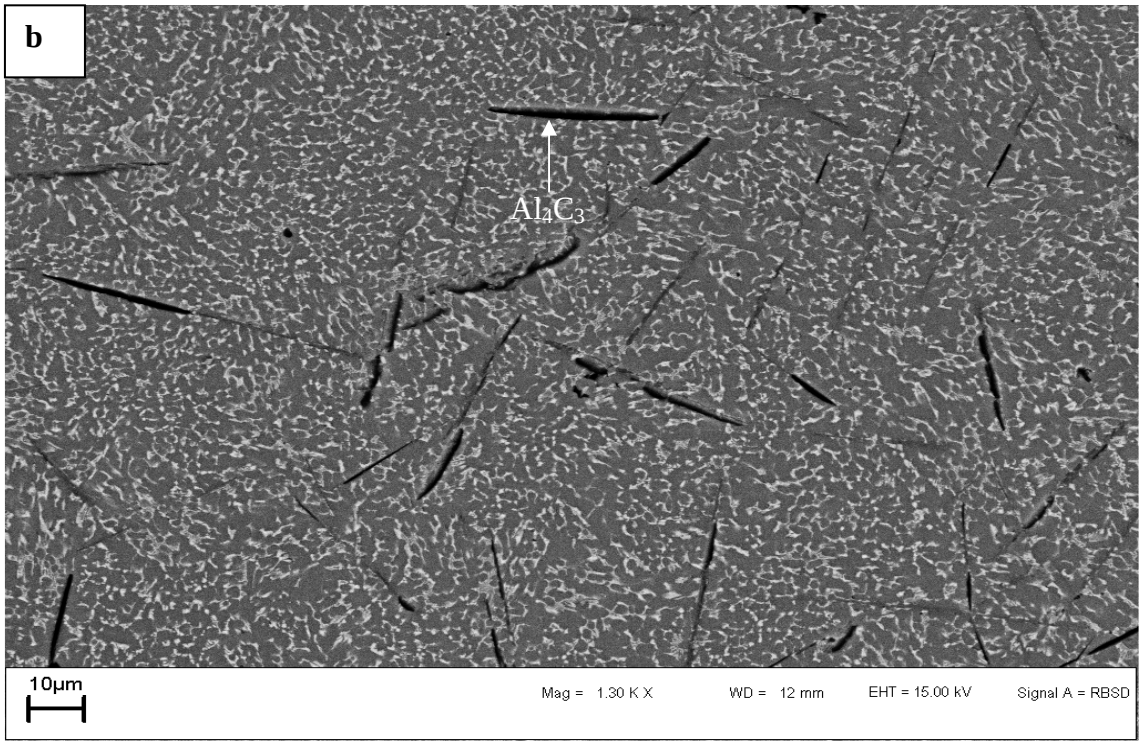
b
Al_4C_3
10µm
Mag = 1.30 K X
WD = 12 mm
EHT = 15.00 kV
Signal A = RBSD

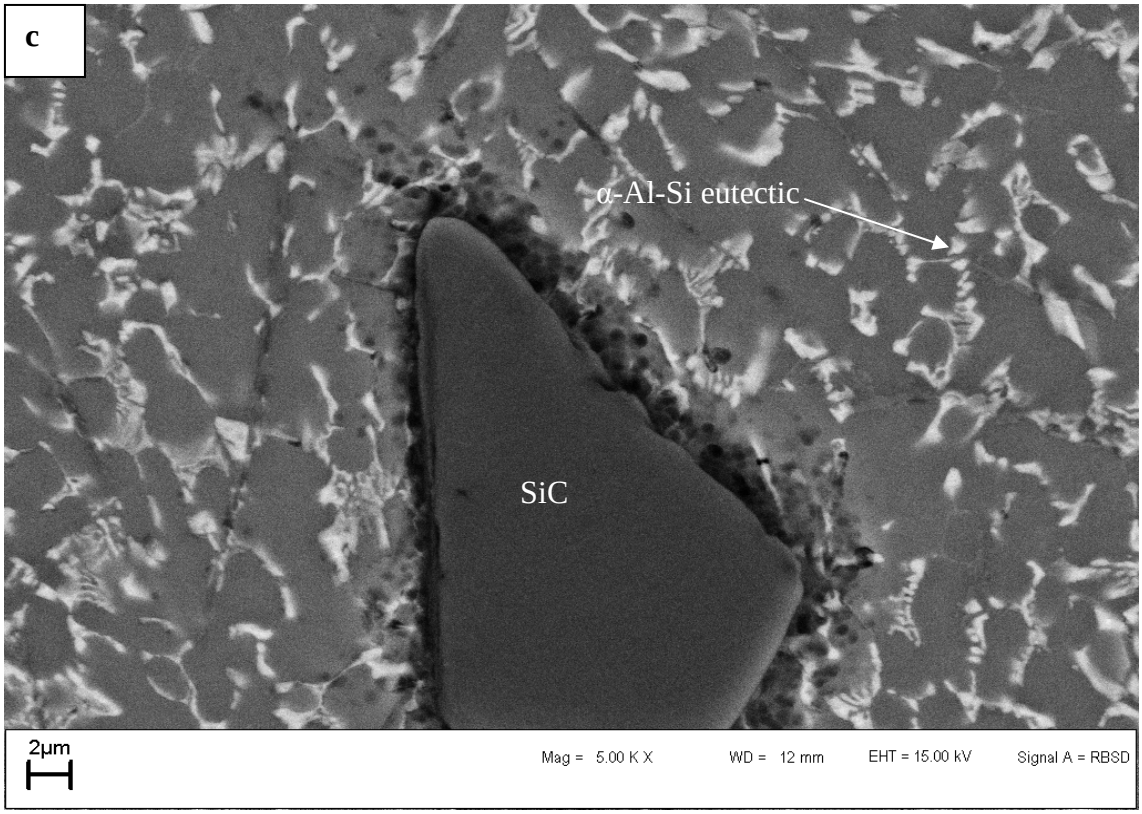

Fig. 10 SEM micrographs of an aluminium surface alloyed with a 70wt%Ni and 30wt%SiC powder showing (a) the alloyed layer with Al_3Ni, (b) and (c) show the microstructure of the heated zone

Figure 11 is the XRD pattern of the alloyed layer showing Al, SiC, Al_3Ni and Al_4C_3 phases. These phases were also observed when alloying with 30wt%Ni and 70wt%SiC.

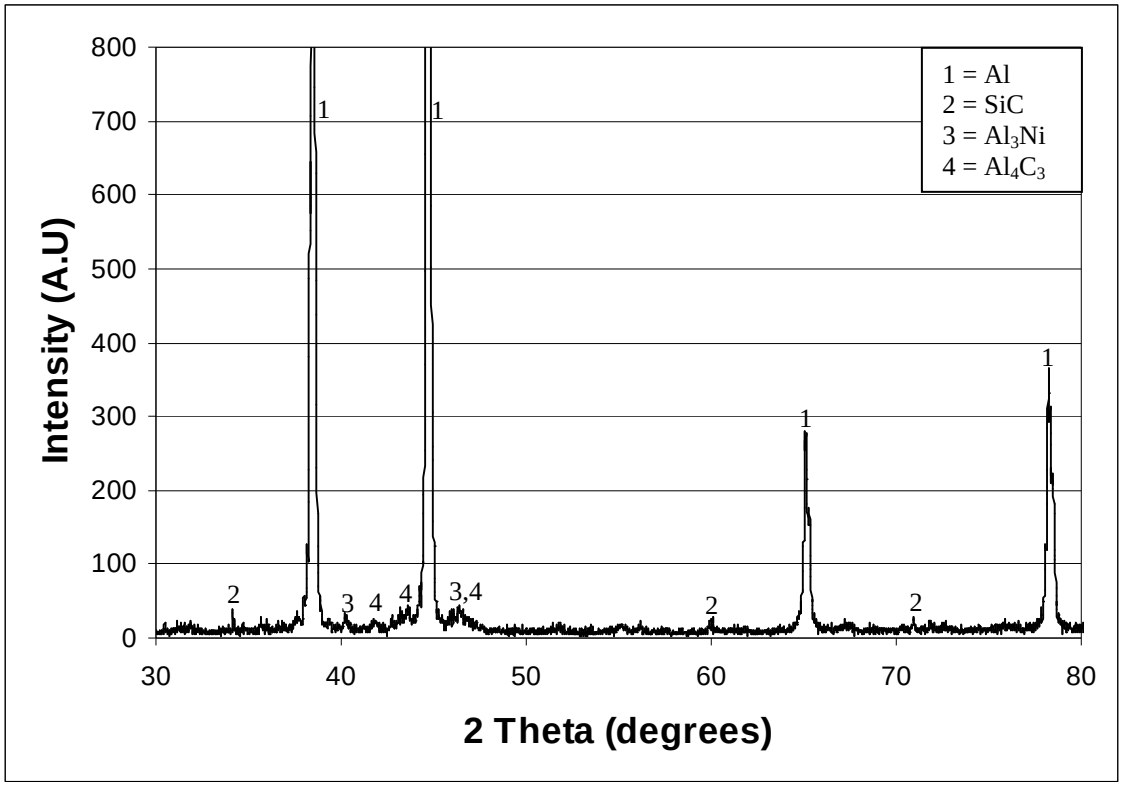

Fig. 11 XRD of an aluminium surface alloyed with 50wt%Ni and 50wt%SiC

3.2.3 70wt% Ni and 30wt%SiC

Figure 12 shows the microstructure of the layer formed by depositing 70wt%Ni and 30wt%SiC in the aluminium matrix. In the alloyed layer depicted in Figure 12(a), the Al_3Ni, Al_4C_3 and α-Al-Si eutectic phases are present. The Al_3Ni intermetallic phase was formed *in situ* during alloying. This intermetallic phase is more dominant in the alloyed layer compared to the Al_4C_3 phase. Alloys with a lower Ni content and a higher SiC content produced more Al_4C_3 phase than Al_3Ni phase. The microstructure in the heated zone is shown in Figure 12(b). In this zone the microstructure was predominately the α-Al-Si eutectic surrounded by the Al matrix. Undissolved SiC particles and the Al_4C_3 phase were also observed. These phases were present in all three alloyed surfaces. These results show that alloying with different powder ratios of Ni and SiC under the selected processing conditions lead to the formation of similar phases in every alloy produced, albeit in varied proportions. The Al_3Ni phase increased as the Ni content increased, while the Al_4C_3 phase was dominant when the SiC content was high.

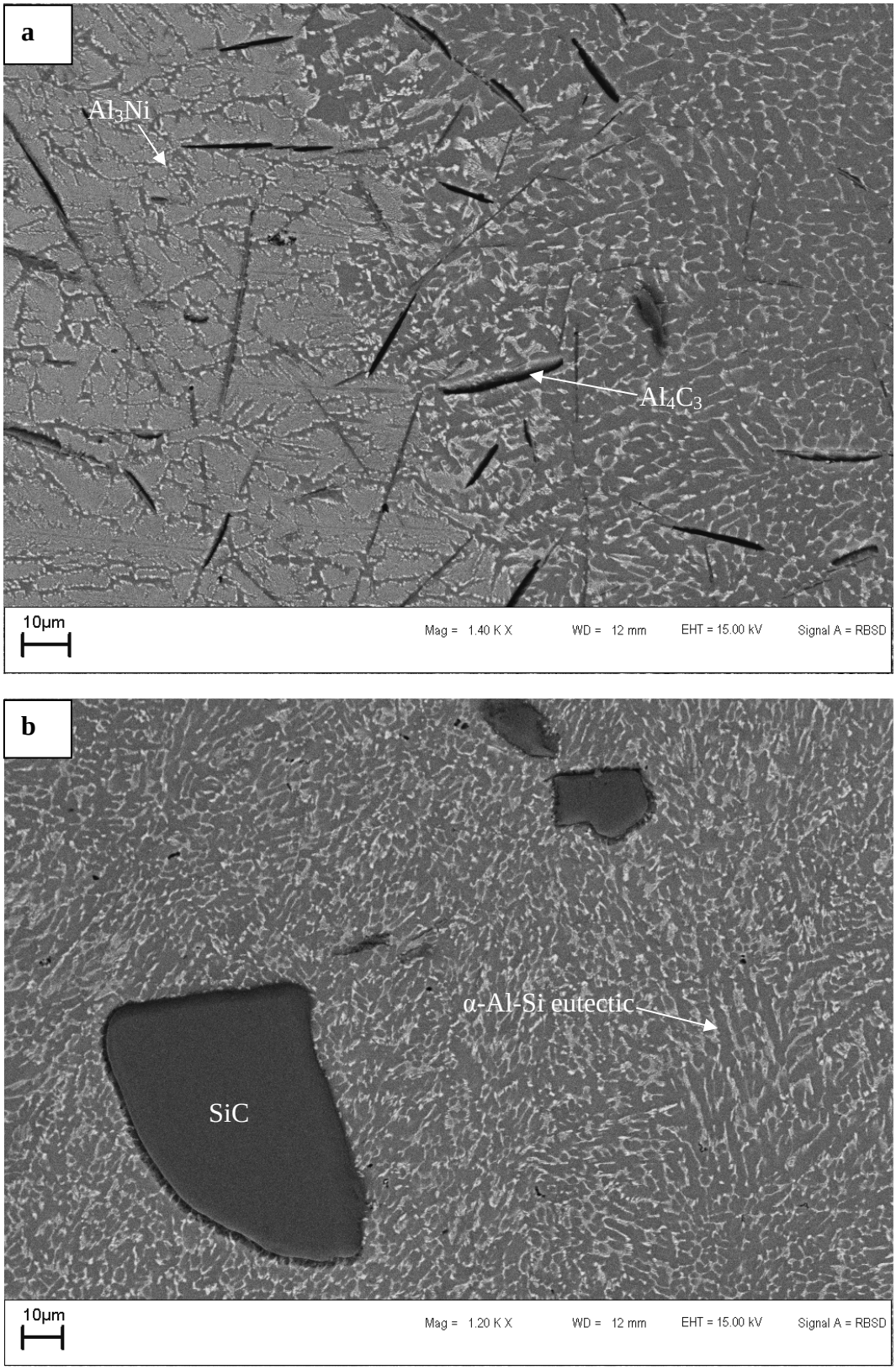

Fig. 12 SEM micrographs of an aluminium surface alloyed with a 70wt% Ni and 30wt% SiC powder showing the microstructures in (a) the alloyed zone and (b) the heated zone

The XRD results of the aluminium alloyed with 70wt%Ni and 30wt%SiC is shown in Figure 13. The phases identified are Al, SiC, Al_3Ni and Al_4C_3. These phases were also found in the previous two alloyed surfaces.

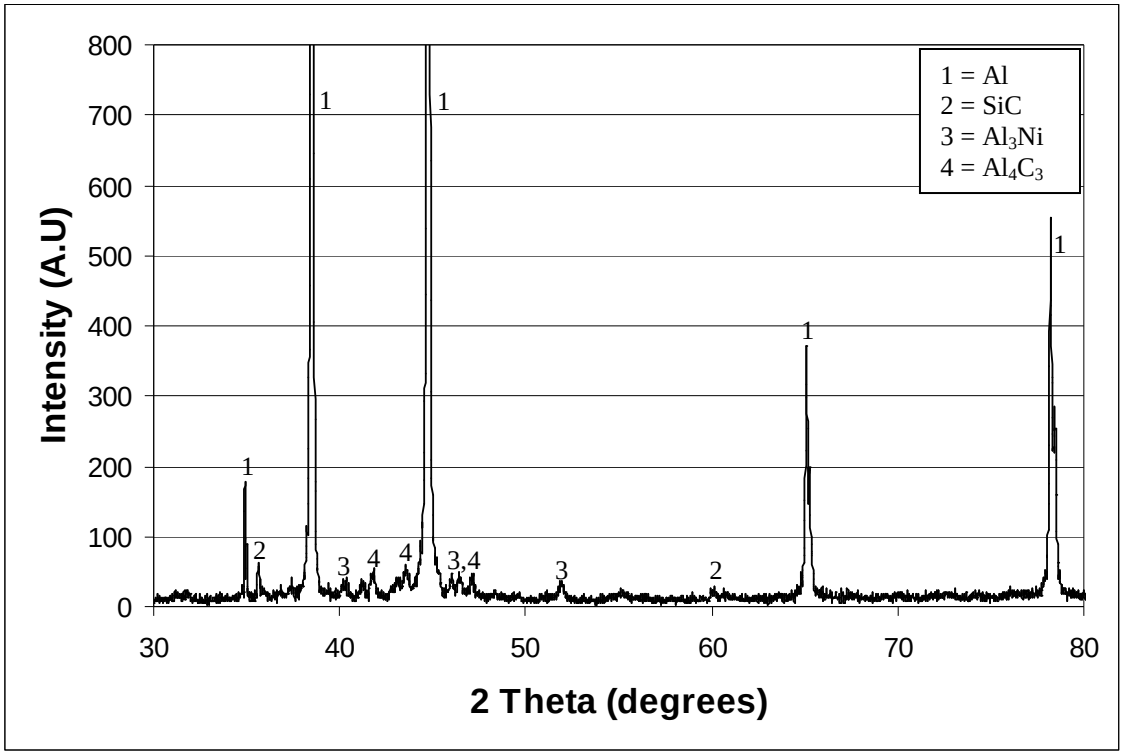

Fig. 13 XRD of an aluminium surface alloyed with 70wt%Ni and 30wt%SiC

The alloyed layers for all three alloys were dominated by the formation of Al_3Ni and Al_4C_3 intermetallic phases. The α-Al-Si eutectic phase was formed between the intermetallic phases. As the Ni content increased and the SiC content decreased, more Al_3Ni phase was formed compared to the Al_4C_3 phase. Fewer SiC particles were available to dissociate and react with Al to form the Al_4C_3 phase when the SiC content decreased and more Ni was available to react with Al and form the Al_3Ni phase when the Ni content increased. The heated zone was dominated by the formation of the α-Al-Si eutectic phase. The Al_3Ni and Al_4C_3 intermetallic phases were formed in the interface region close to the alloyed layer. This region was between 0.7mm and 1.2mm from the surface of the alloyed layer. Deeper than 1.2mm, the α-Al-Si eutectic phase, few intermetallic phases and few SiC particles were observed in the alloyed materials. Few undissloved SiC particles were found in the alloyed layer and the heated zone.

3.3 Hardness

The hardness profiles for the three alloyed surfaces are shown in Figure 14. Laser alloying with a mixed Ni and SiC powder resulted in an increase in hardness of the alloyed zone to approximately 4 times that of the aluminium alloy substrate. For the heated zone, the increase in hardness was approximately 2 times that of the aluminium alloy substrate. The high hardness of the alloyed layers is attributed to the formation of intermetallic phases (Al_4C_3 and Al_3Ni) during alloying. In the heated zone, the formation of the α-Al-Si eutectic resulted in the increase in hardness. Few Al_4C_3 and Al_3Ni phases formed in this region compared to the alloyed layer.

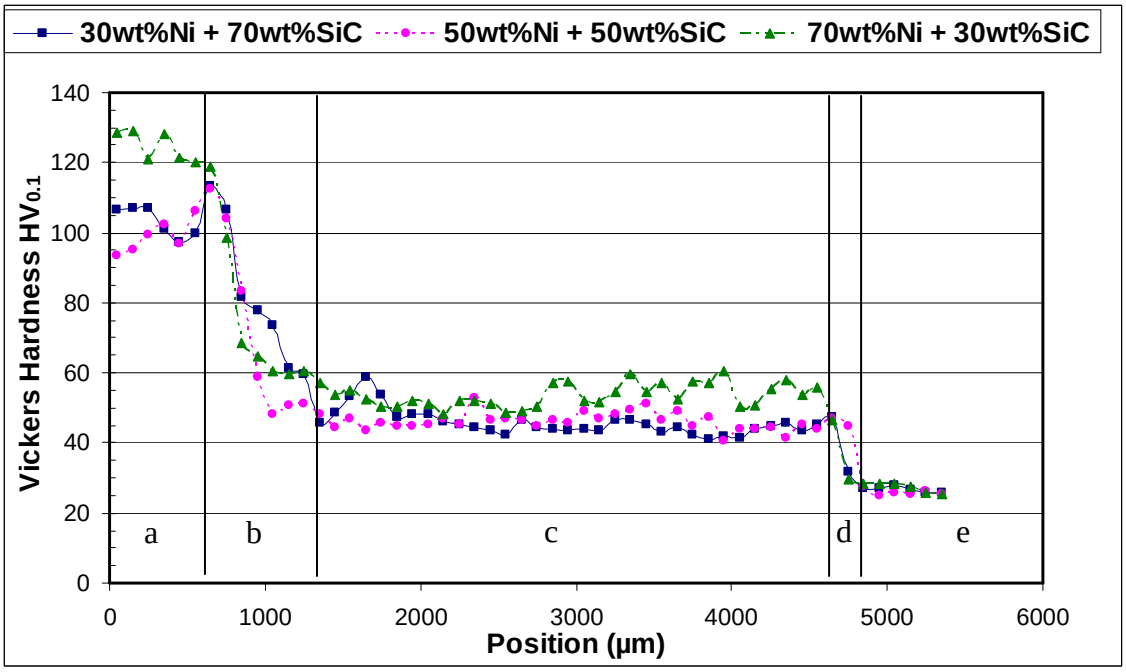

Fig. 14 Comparison of hardness profiles. (a) is the alloyed layer, (b) is the interface between the alloyed layer and the heated zone, (c) is the heated zone, (d) is the interface between the heated zone and the Al substrate and (e) is the Al substrate

The hardness results for the alloyed layers are given in Table 3. Increasing the Ni content and decreasing the SiC content did not have a significant impact on the hardness values.

Table 3 Hardness of the alloyed and heated zones.

Powder Composition	Alloyed zone ($HV_{0.1}$)	Heated zone ($HV_{0.1}$)
30wt%Ni + 70wt%SiC	104.8 ± 5.2	48.1 ± 8.2
50wt%Ni + 50wt%SiC	101.2 ± 6.3	46.8 ± 3.3
70wt%Ni + 30wt%SiC	120.7 ± 9.8	54.2 ± 4.1

4. Conclusions

Laser alloying aluminium AA1200 with a powder containing Ni and SiC results in an increase in surface hardness. Two zones were observed in the alloyed microstructure. The alloyed zone formed at the surface and was dominated by the formation of Al_4C_3 and Al_3Ni phases. The heated zone formed between the alloyed zone and the aluminium substrate and was dominated by the formation of an α-Al-Si eutectic phase. Few undissolved SiC particles were observed in both zones. The hardness of the alloyed zone was higher than the hardness of the heated zone due to the differences in the phase proportions achieved. As the Ni content increased and the SiC content decreased, more Al_3Ni formed compared to Al_4C_3. A hardness increase of approximately 4 times in the alloyed zone and 2 times in the heated zone was achieved after laser alloying with Ni and SiC powders.

Acknowledgements

The Department of Science and Technology and the Centre for Scientific and Industrial Research are acknowledged for financial support.

References

[1] Riabkina-Fisherman M, Zahavi J (1996), Laser alloying and cladding for improving surface properties, Applied Surface Science 106: 263-267.

[2] Ravi N, Sastikumar D, Subramanian N, Nath AK, Masilamani V (2000), Microhardness and microstructure studies on laser surface alloyed aluminium alloy with Ni-Cr, Materials and Manufacturing Processes, 15: 395-404.

[3] Wong TT, Liang GY, Tang CY(1997), The surface character and substructure of aluminium alloys by laser-melting treatment, Journal of Materials Processing Technology, 66: 172-178.

[4] Bysakh S, Mitra SK, Phanikumar G, Mazumder J, Dutta P, Chattopadhyay K (2003), Characterization of microstructure in laser-surface-alloyed layers of aluminium on nickel, Metallurgical and Materials Transactions A 34A: 2621-2631.

[5] Goral M, Moskal G, Swadzba L, Tetsui T (2007), Si-modified aluminium coating deposited on TiAlNb alloy by slurry method, Journal of Achievements in Materials and Manufacturing Engineering, 21: 75-78.

[6] Hu C, Xin H, Baker TN (1996), Formation of continuous surface Al-SiCp metal matrix composite by overlapping laser tracks on AA6061 alloy, Materials Science and Technology, 12: 227 - 232.

[7] Kaczmar JW, Pietrzak K, Włosiński W (2000), The production and application of metal matrix composite materials, Journal of Materials Processing Technology, 106: 58-67.

[8] Gingu O, Mangra M, Orban RL (1999), In-situ production of Al/SiCp composite by laser deposition technology, Journal of Materials Processing Technology, 89-90: 187-190.

[9] Su R, Lei Y (2008), Microstructure and hardness of laser clad SiC_p-Al composite coatings on Al alloys, Materials Letters, 62: 3272 - 3275.

[10] Hu C, Baker TN (1997), A new aluminium silicon carbide formed in laser processing, Journal of Materials Science, 32: 5047-5051.

[11] Wieczorek J, Dolata-Grosz A, Dyzia M, Śleziona J (2006), Tribological properties of aluminium matrix composite reinforced with intermetallic, Journal of Achievements in Materials and Manufacturing Engineering, 15: 58-62.

[12] Dutta Majumder J, Chandra BR, Nath AK, Manna I (2008), Studies on compositionally graded silicon carbide dispersed composite surface on mild steel developed by laser surface cladding, Journal of Materials Processing Technology, 203: 505-512.

[13] Adamiak M (2006), Selected properties of the aluminium alloy base composite reinforced with intermetallic particles, Journal of Achievements in Materials and Manufacturing Engineering, 14: 43-47.

[14] Anandkumar R, Almeida A, Colaço R, Vilar R, Ocelik V, De Hosson JThM. (2007), Microstructure and wear studies of laser clad Al-Si/$SiC_{(p)}$ composite coatings, Surface and Coating Technology, 201: 9497-9505.

[15] Leon-Patiño CA, Drew RAL(2005), Role of metal interlayers in the infiltration of metal-ceramic composites, Current Opinion in Solid State and materials Science, 9: 211-218.

[16] Selvan JS, Soundararajan G, Subramanian K (2000), Laser alloying of aluminium with electrodeposited nickel: optimization of plating thickness and processing parameters, Surface and Coatings Technology, 124: 117-127.